ChemComm

Accepted Manuscript

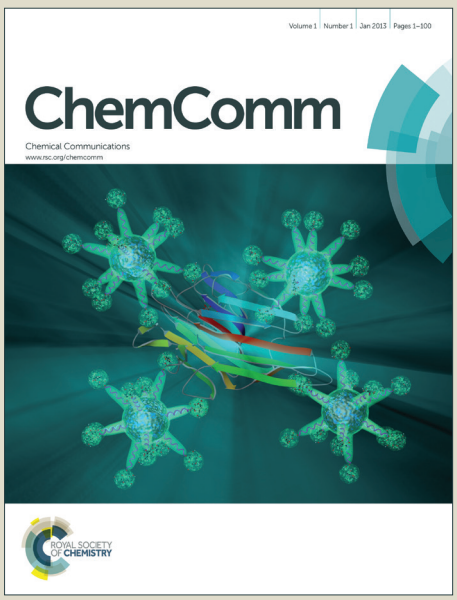

ROYAL SOCIETY OF CHEMISTRY

www.rsc.org/chemcomm

ChemComm

COMMUNICATION

Versatile Thermally Activated Delayed Fluorescence Emitter for Both Highly Efficient Doped and Non-Doped Organic Light Emitting Devices

Received 00th January 2015,
Accepted 00th January 20xx

DOI: 10.1039/x0xx00000x

www.rsc.org/

Wei-Lung Tsai,[a] Ming-Hao Huang,[b] Wei-Kai Lee,[a] Yi-Jiun Hsu,[a] Kuan-Chung Pan,[a] Yi-Hsiang Huang,[a] Hao-Chun Ting,[b] Monima Sarma,[b] Yu-Yi Ho,[b] Hung-Chieh Hu,[c] Chung-Chia Chen,[c] Meng-Ting Lee,[c] Ken-Tsung Wong*[b] and Chung-Chih Wu*[a]

A thermally activated delayed fluorescent (TADF) emitter (DMAC-TRZ) was reporetd either as the emitting dopant in a host or as the non-doped (neat) emitting layer to achieve high EL EQEs of up to 26.5% and 20% in OLEDs, respectively.

Due to the nature of exciton formation through carrier recombination, most of excitons (~75%) formed in organic light-emitting devices (OLEDs) are initially triplet excitons.[1] Thus to achieve ideally 100% internal quantum efficiency OLEDs, effective channels must be established to make efficient use of the otherwise non-emissive triplet excitons for efficient electroluminescence (EL). Phosphorescent emitters incorporating transition metals in the organic aromatic frameworks to facilitate efficient triplet-state emission have been successful in achieving this.[1-3] The recent development of efficient thermally activated delayed fluorescent (TADF) emitters based on purely organic aromatic frameworks,[4-6] which have reduced energy gaps between singlet and triplet excited states (i.e., ΔE_{ST}) and thus efficient reverse intersystem crossing (RISC) for harvesting triplet excitons to give effective delayed fluorescence,[4-6] is also becoming attractive due to the avoidance of rare and more expensive transition metals and potential cost advantages. Rather high EL external quantum efficiencies (EQEs) around 20% photons/electrons have been demonstrated in OLEDs employing TADF emitters.[6-11]

To avoid general concentration quenching and to ensure high emission efficiency, high-efficiency OLEDs of all different emission mechanisms in general adopt the host-guest emitting layers that incorporate emitters as emitting dopants (guests) in appropriate host matrices.[1-11] However, for efficient OLEDs generally fabricated by vacuum deposition, the host-guest configurations for emitting layers require high-precision control of host-guest co-evaporation, complicating the device structure, device fabrication, and deposition facility. To simplify the device structure/fabrication and to reduce fabrication cost, it would be desirable that efficient OLEDs could be made with non-doped (neat) emitting layers. However, up to date, reports of decently efficient OLEDs using neat (non-doped) emitting layers are still generally rare.[12-15]

Here in this work, we report a TADF emitter that not only shows prominent TADF and high photoluminescence quantum yield (PLQY) as the dopant in a host but also preserves such distinct characteristics in non-doped (neat) films. High EL EQEs of up to 26.5% and 20% have been achieved in OLEDs using such a TADF emitter either as the emitting dopant in a host or as the non-doped (neat) emitting layer, respectively. Such characteristics of a TADF emitter shall render it versatile for applications in different device configurations, for achieving high efficiency, device/fabrication simplification, and/or cost reduction simultaneously.

The molecular material **DMAC-TRZ** under investigation is shown in **Fig. 1a**. It adopts the general donor-acceptor (D-A) molecular architecture of TADF emitters,[5-11] with 9,9-dimethyl-9,10-dihydroacridine (DMAC) as the electron-donor moiety and 2,4,6-triphenyl-1,3,5-triazine (TRZ) as the electron-acceptor moiety. This molecule was derived from a known TADF molecule **PXZ-TRZ** (Fig. 1a),[7] by replacing the phenoxazine (PXZ) donor unit with the DMAC. Although all PXZ, DMAC, and TRZ are known donor or acceptor moieties for the D-A-type TADF molecules in recent years,[7,9] yet we notice that the combination of DMAC and TRZ (and thus the **DMAC-TRZ** molecule) has not been reported. Phtophysical characterizations also reveal its superior and unique TADF emission characteristics compared to **PXZ-TRZ**.

DMAC-TRZ was obtained in 92% yield as 9,9-dimethyl-9,10-dihydroacridine reacted with 2-(4-bromophenyl)-4,6-diphenyl-1,3,5-triazine and refluxed in toluene for 48 h in the presence of Pd catalyst. **DMAC-TRZ** was fully characterized using ^{1}H and ^{13}C NMR spectroscopy, mass spectrometry, and elemental analysis. Scheme S1 in Electronic Supplementary Information (ESI) illustrates the synthesis of **DMAC-TRZ**.

[a] Department of Electrical Engineering, Graduate Institute of Electronics Engineering, and Graduate Institute of Photonics and Optoelectronics, and Innovative Photonics Advanced Research Center (i-PARC), National Taiwan University, Taipei 10617, Taiwan. E-mail: wucc@ntu.edu.tw.
[b] Department of Chemistry, National Taiwan University, and Institute of Atomic and Molecular Science, Academia Sinica,Taipei 10617, Taiwan. E-mail: kenwong@ntu.edu.tw.
[c] AU Optronics Corp., Hsinchu 30078, Taiwan.

† Electronic Supplementary Information (ESI) available: experimental details, synthesis and structural charcterizations, UV-vis and emission spectra, cyclic voltammogram. See DOI: 10.1039/x0xx00000x

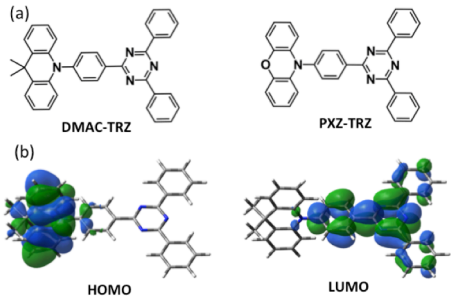

Fig. 1. (a) Molecular structures of **DMAC-TRZ** and **PXZ-TRZ**. (b) Calculated spatial distributions of HOMO and LUMO of **DMAC-TRZ**.

Fig. 1b shows spatial distributions of highest occupied molecular orbital (HOMO) and lowest unoccupied molecular orbital (LUMO) of **DMAC-TRZ**, calculated with the Gaussian 09 package at the B3LYP/6-311G(d) level, using the time-dependent density function theory (TD-DFT) for the geometry optimizations. Similar to the case of **PXZ-TRZ**,[7] a twisted configuration (with a relatively large dihedral angle of 88°) occurs between acridine donor and triphenyltriazine acceptor moieties, beneficial for breaking their conjugation. With HOMO and LUMO locating mainly on the DMAC and TRZ moieties, respectively, the effective separation between HOMO and LUMO is believed to be beneficial for reducing ΔE_{ST} for efficient RISC,[5-11] as confirmed by measured small ΔE_{ST} and distinct TADF behaviors to be discussed below.

The thermal and morphological properties of **DMAC-TRZ** were characterized using thermogravimetric analysis (TGA) and differential scanning calorimetry (DSC). In TGA, **DMAC-TRZ** shows high thermal stability with a decomposition temperature of 305 °C (T_d, corresponding to 5 % weight loss). In DSC, **DMAC-TRZ** exhibits a distinct glass transition at 91 °C, higher than that of **PXZ-TRZ** and ensuring formation of stable amorphous neat films of **DMAC-TRZ** by vacuum deposition.

Fig. 2a depicts the UV-Vis absorption spectrum of **DMAC-TRZ** in solution (toluene), and its fluorescence spectrum (measured at room temperature) and phosphorescence spectrum (measured at 77 K) when doped (with a doping concentration of 8 wt.%) in a large-triplet-energy host mCPCN [9-(3-(9*H*-carbazol-9-yl)phenyl)-9*H*-carbazole-3-carbonitrile].[13] The strong absorption of **DMAC-TRZ** around 300 nm could be assigned to the π-π* transition, while the weak absorption band around 350-450 nm is attributed to the intramolecular charge-transfer (ICT) transition from the DMAC moiety to the TRZ moiety. The fluorescence and phosphorescence of **DMAC-TRZ** in doped films give broad and structureless spectra centering at 495 nm and 504 nm, respectively (Table 1). Compared to **PXZ-TRZ**, **DMAC-TRZ** shows a much blue-shifted absorption and emission in a same solvent or host (Table 1, also see Fig. S1 and Fig. S2 in ESI for various photophysical properties of **PXZ-TRZ**), in replacing PXZ with the weaker electron-donating group DMAC. The ICT nature of the electronic transitions in **DMAC-TRZ** can be further manifested by the evident solvatochromic behavior of **DMAC-TRZ**'s fluorescence in solvents of different polarity (see ESI, Fig. S3).[9] From the difference in the onset wavelengths of fluorescence and phosphorescence spectra, a relatively small ΔE_{ST} of ~46 meV is

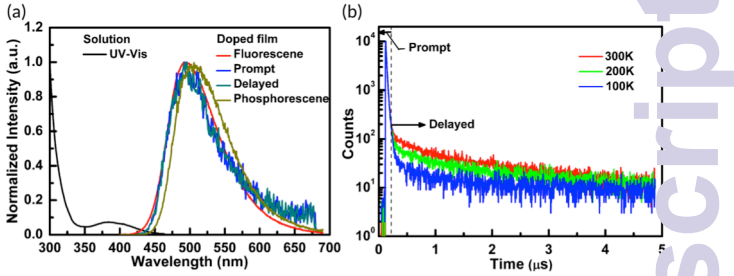

Fig. 2. (a) UV-Vis absorption spectrum of **DMAC-TRZ** in solution (toluene), and steady-state fluorescence spectrum, spectra of the prompt and delayed components in transient PL, (all measured at room temperature), and phosphorescence spectrum (measured at 77 K) of **DMAC-TRZ** doped in mCPCN films (with a doping concentration of 8 wt.%). (b) PL decay cruves of **DMAC-TRZ**-doped films measured at various temperatures.

extracted for **DMAC-TRZ** (Table 1), indicating possibility of TADF in **DMAC-TRZ**. Indeed, the transient photoluminescence (PL) (Fig. 2b) of **DMAC-TRZ** in the mCPCN host measured at room temperature clearly exhibits a delayed component (with a lifetime of 1.89 μs, Table 1) following a prompt component (with a lifetime of 20.3 ns, Table 1). The PL spectrum collected for the delayed component (Fig. 2a) coincides well with both the spectrum of the prompt component and the steady-state PL spectrum, confirmming it is indeed delayed fluorescence. Together with the evident drop of the delayed component in lowering the temperature (Fig. 2b), it can be clearly assigned as TADF. At room temperature, **DMAC-TRZ** doped in mCPCN exhibits a rather high PLQY of ~90% (Table 1), superior to 66% of **PXZ-TRZ**. As estimated from the PL decay curve, the delayed component accounts for ~34% of the total fluorescence from **DMAC-TRZ**, whereas the emission of **PXZ-TRZ** comprises ~29% delayed fluorescence (Table S2). Obviously, the model molecule **PXZ-TRZ** exhibits inferior PLQYs both in prompt and delayed fluorescence, implying occurring of more prominent non-radiative processes in the excited states possibly due to its intrinsic stronger ICT character.

As shown in Fig. 3a/3b and Table 1, neat films of **DMAC-TRZ** exhibit photophysical and TADF properties rather similar to those of **DMAC-TRZ** doped in host films, except for slight red shifts (~10 nm) in fluorescence, delayed fluorescence and phosphorescence spectra.

Table 1. The summary of physical and photophysical properties of **DMAC-TRZ** and **PXZ-TRZ**.

	DMAC-TRZ		PXZ-TRZ	
	Doped	Neat	Doped	Neat
$\lambda_{max,\ abs}$ [b] [nm]	390[a]	390	425[a]	430
$\lambda_{max,\ fl}$ [c] [nm]	495	500	540	560
$\lambda_{max,\ ph}$ [d] [nm]	504	510	535	55
ΔE_{ST} [meV]	46	50	16.8	2
PLQY [%]	90	83	66	4
τ_{prompt} [e] [ns]	20.3	26.3	20	21.8
τ_{delay} [f] [μs]	1.9	3.6	1.1	1.2

[a] Measured in toluene solution. [b] absorption maximum wavelength. [c] fluorescence maximum wavelength. [d] phosphorescence maximum wavelength. [e] lifetime of the prompt component in transient PL. [f] lifetime of the delayed component in transient PL.

(perhaps due to difference in the polarity of surrounding media) and slight changes in lifetimes for both prompt and delayed fluorescence. The most intriguing feature, however, is that **DMAC-TRZ** neat films retain a rather high PLQY of ~83% (in which delayed fluorescence accounts for ~38-40% of the total fluorescence), revealing significantly suppressed concentration quenching.

As a comparison, the PLQY of **PXZ-TRZ** drops from 66% of the doped film to only 43% of the neat film. Previous studies indicate the π–π stacking of the PXZ donors would quench the emission of PXZ–contained compounds in neat films.[7] For neat films of DMAC–TRZ, the methyl groups on the steric SP^3 C of DMAC units might be beneficial to inhibit the interaction between donors, leading to a high PLQY in neat films. Previously, due to general concentration quenching of emission from TADF materials, to achieve/retain high emission efficiency, it is general to use TADF emitters as emitting dopants.[5-11] High PLQY and low concentration quenching simultaneously achieved with the TADF emitter here suggest that it may be useful for technically attractive non-doped TADF OLEDs, in addition to doped device applications.

The electrochemical properties of **DMAC-TRZ** were investigated by cyclic voltammetry (CV). The cyclic voltammograms of both **DMAC-TRZ** and **PXZ-TRZ** are shown in Fig. S4. Similar to **PXZ-TRZ**, **DMAC-TRZ** shows promising bipolar electrochemical properties with good reversibility in both the oxidation and the reduction scans. As seen in the cyclic voltammogram, the introduction of DMAC leads to slightly higher oxidation potential and thus slightly deeper HOMO level (while keeping reduction potential and LUMO level more or less intact), enlarging the energy gap. The electrochemical results indicate that **DMAC-TRZ** possesses promising electrochemical stability and bipolar characteristics, which may be particularly beneficial to devices using **DMAC-TRZ** as the non-doped emitting layer.

Since **DMAC-TRZ** exhibits efficient TADF both in doped films and non-doped (neat) films, OLEDs using **DMAC-TAZ** either as the emitting dopant in a host or as the non-doped (neat) emitting layer were studied. The doped device had the structure of: glass substrate/ITO anode/PEDOT:PSS (70 nm)/TAPC (15 nm)/mCP (5 nm)/mCPCN:**DMAC-TRZ** 8 wt.% (20 nm)/DPPS (5 nm)/3TPYMB (45 nm)/LiF (0.5 nm)/Al (150 nm). The non-doped device had the structure of: glass substrate/ITO anode/PEDOT:PSS (70 nm)/TAPC (10 nm)/mCP (10 nm)/**DMAC-TRZ** (20 nm)/DPPS (5 nm)/3TPYMB (45 nm)/LiF (0.5 nm)/Al (150 nm). The transparent conducting polymer poly(3,4-ethylenedioxythiophene):poly(styrenesulfonate) (PEDOT:PSS) served as the hole-injection layer.[16,17] Di-[4-(N,N-ditolyl-amino)-phenyl]-cyclohexane (TAPC) and N,N-dicarbazolyl-3,5-benzene (mCP) were hole-transport layers,[16] while diphenyl-bis[4-(pyridin-3-yl)phenyl]silane (DPPS) and tris-[3-(3-pyridyl)mesityl]borane (3TPYMB) were the hole-blocking and electron-transport layers.[16,18] mCPCN doped with 8wt.% DMAC-TRZ or the neat DMAC-TRZ layer was the emitting layer. LiF and Al were the electron injection layer and the cathode, respectively.[16,17] Molecular structures of various materials used in devices and energy-level diagrams for doped and non-doped device are shown in Figure S5 and S6, respectively (see ESI). PEDOT:PSS films were prepared by spin-coating from an aqueous dispersion of PEDOT:PSS (Clevios, Heraeus Co.), followed by annealing on a hot plate at 130 °C for 15 min. under ambient conditions. All other layers above the

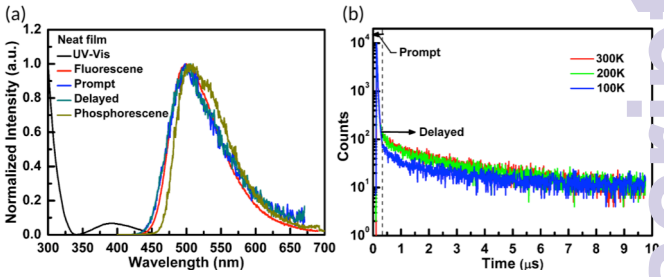

Fig. 3. (a) UV-Vis absorption spectrum, steady-state fluorescence spectrum, spectra of the prompt and delayed components in transient PL (all measured at room temperature), and phosphorescence spectrum (measured at 77 K) of **DMAC-TRZ** neat films. (b) PL decay cruves of **DMAC-TRZ** neat films measured at various temperatures.

ITO and PEDOT:PSS were deposited by thermal evaporation and were defined by in-situ shadow masking (typically with an active area of 1 mm^2).

Fig. 4 shows the EL characteristics of the doped and non-doped devices, which are also summarized in Table 2. The EL spectra (Fig. 4a) of both devices are similar to their corresponding PL spectra in thin films (i.e., blue-green to green emission and a slight red shift in the EL spectrum of the non-doped device), indicating pure EL from either **DMAC-TRZ** dopants or **DMAC-TRZ** neat films. Both devices exhibit similar I-V characteristics, with a turn-on voltage of ~ 3 V (defined as the voltage when the luminance becomes detectable).

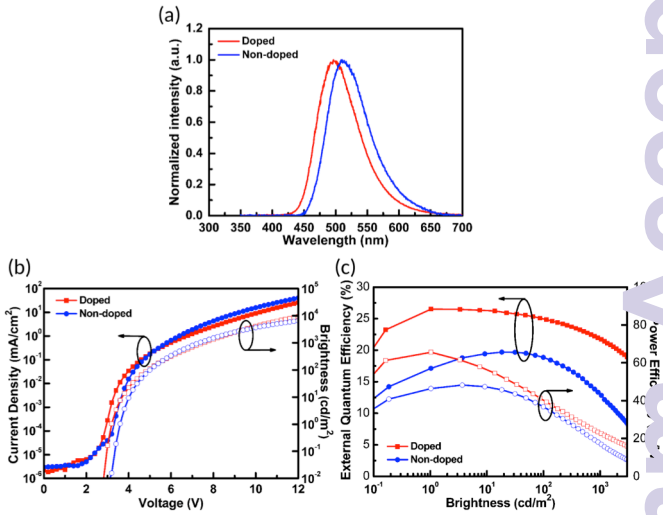

Figure 4. (a) EL spectra, (b) current-voltage-luminance (I-V-L) characteristics, and (c) external quantum efficiency and pwoer efficiency of doped and non-doped devices.

Table 2. The summary of OLED characteristics.

	External quantum efficiency [%]	Current efficiency [cd A^{-1}]	Power efficiency [lm W^{-1}]
Doped			
peak	26.5	66.8	65.6
100 cd m^{-2}	25.1	63.2	41.4
Non-doped			
Peak	20	61.1	45.7
100 cd m^{-2}	18.9	58.6	36.8

and low operation voltage (e.g. ~ 4.5 V for a practical brightness of 100 cd m^{-2}). Such I-V characteristics suggest decent charge-transport properties in **DMAC-TRZ** neat films, as alreadysuggested by electrochemical characterization. Large and balanced currents in hole-only and electron-only single-carrier devices also indicate excellent bipolar charge transport properties of DMAC-TRZ (see ESI, Figure S7). Both devices show promisingly high EL efficiencies. The doped device gives an external quantum efficiency, current efficiency and power efficiency of up to (26.5%, 66.8 cd A^{-1}, 65.6 lm W^{-1}). Most importantly, even the non-doped device gives impressive external quantum efficiency, current efficiency and power efficiency of up to (20%, 61.1 cd A^{-1}, 45.7 lm W^{-1}), which are comparable to those of doped devices. To our knowledge, quantum efficiencies of the present doped **DMAC-TRZ** device are among the highest ever reported for TADF OLEDs and are comparable to those of state-of-the-art phosphorescent OLEDs.[2,3,6-11] Meanwhile those of the non-doped **DMAC-TRZ** device are also among the highest ever reported for non-doped OLEDs of all different emission mechanisms.[12-15] The demonstration of both highly efficient doped and non-doped OLEDs from a same TADF emitter shall render it versatile for applications in different device configurations, for achieving high efficiency, device/fabrication simplification, and/or cost reduction.

In summary, we report an efficient TADF emitter (**DMAC-TRZ**) that not only shows high PLQY (≥90%) in doped films but also possesses low concentration quenching and high PLQY (83%) in neat films. As a result, highly efficient TADF OLEDs (with EQE of 26.5%) was implemented using **DMAC-TRZ** as the emitting dopant and comparable EL efficiency (with EQE of 20%) had also been achieved by using it as the non-doped (neat) emitting layer. EL efficiencies of the present doped **DMAC-TRZ** device are among the highest ever reported for TADF OLEDs and are comparable to those of state-of-the-art phosphorescent OLEDs. Meanwhile those of the non-doped **DMAC-TRZ** device are also among the highest ever reported for non-doped OLEDs of all different emission mechanisms. The demonstration of both highly efficient doped and non-doped OLEDs from a same TADF emitter shall render it versatile for applications in different device configurations, for achieving high efficiency, device/fabrication simplification, and/or cost reduction.

Notes and references

1 M. A. Baldo, D. F. O'Brien, Y. You, A. Shoustikov, M. E. Thompson and S. R. Forrest, *Nature,* 1998, **395**, 151-154.
2 C. Fan, C. Yang, *Chem. Soc. Rev.*, 2014, **43**, 6439-6469.
3 S. Gong, Y. Chen, J. Luo, C. Yang, C. Zhong, J. Qin, D. Ma, *Adv. Funct. Mater.*, 2011, **21**, 1168-1178.
4 A. Endo, M. Ogasawara, A. Takahashi, D. Yokoyama, Y. Kato and C. Adachi, *Adv. Mater.*, 2009, **21**, 4802-4806.
5 T. Nakagawa, S.-Y. Ku, K.-.T. Wong and C. Adachi, *Chem. Commun.*, 2012, **48**, 9580-9582.
6 H. Uoyama, K. Goushi, K. Shizu, H. Nomura and C. Adachi, *Nature*, 2012, **492**, 234-238.
7 H. Tanaka, K. Shizu, H. Miyasaki and C. Adachi, *Chem. Commun.*, 2012, **48**, 11392-11394.
8 H. Wang, L. Xie, Q. Peng, L. Meng, Y. Wang, Y. Yi and P. Wang, *Adv. Mater.*, 2014, **26**, 5198-5204.
9 Q. Zhang, Bo. Li, S. Huang, H. Nomura, H. Tanaka and C. Adachi, *Nature Photonics*, 2014, **8**, 326-332.
10 J.-I. Nishide, H. Nakanotani, Y. Hiraga and C. Adachi, *Appl. Phys. Lett.*, 2014, **104**, 233304.
11 B. S. Kim and J. Y. Lee, *Adv. Funct. Mater.*, 2014, 24, 3970-3977.
12 C.-C. Wu, Y.-T. Lin, K.-T. Wong, R.-T. Chen and Y.-Y. Chien, *Adv. Mater.*, 2004, **16**, 61-65.
13 Q. Wang, L. W. H. Oswald, X. Yang, G. Zhou, H. Jia, Q. Qiao, Y. Chen, J. Hoshikawa-Halbert and B. E. Gnade, *Adv. Mater.*, 2014, **26**, 8107-8113.
14 Q. Zhang, D. Tsang, H. Kuwabara, Y. Hatae, B. Li, T. Takahashi, Y. Lee, T. Yasuda and C. Adachi, *Adv. Mater.*, 2015, **27**, 2096-2100.
15 K. Albrecht, K. Matsuoka, K. Fujita and K. Yamamoto, *Angew. Chemie.*, 2015, **127**, 5769-5774.
16 M.-S. Lin, S.-J. Yang, H.-W. Chang, Y.-H. Huang, Y.-T. Tsai, C. C. Wu, S.-H. Chou, E. Mondal and K.-T. Wong, *J. Mater. Chem.*, 2012, **22**, 16114-16120.
17 C.-C. Wu, Y.-T. Lin, K.-T. Wong, R.-T. Chen and Y.-Y. Chien, *Adv. Mater.*, 2004, **16**, 61-65.
18 L. Xiao, Z. Chen, B. Qu, J. Luo, S. Kong, Q. Gong and J. Kido, *Adv. Mater.*, 2011, **23**, 926-952.